ACS OMEGA

Open Access

http://pubs.acs.org/journal/acsodf

Article

Peptide Family Promotes Brain Cell Rejuvenation and Improved Cognition through Peripheral Delivery

Alejandro Anton-Fernandez, Indalo Domene-Serrano, Raquel Cuadros, Rocio Peinado-Cahuchola, Margarita Sanchez-Pece, Felix Hernandez, and Jesus Avila*

Cite This: *ACS Omega* 2025, 10, 13236−13250

Read Online

ACCESS | Metrics & More | Article Recommendations | Supporting Information

ABSTRACT: Ligands targeting folate receptor α (FRα), a protein predominantly expressed in neural cells, have the potential to reprogram (rejuvenate) brain cells and enhance cognitive function in aged mice. In this study, we present a family of FRα-binding peptides identified through AlphaFold modeling. These peptides induce a structural change in the receptor upon binding, which facilitates its internalization and transport to the cell nucleus. Once in the nucleus, FRα functions as a transcription factor, promoting the expression of genes associated with a youthful phenotype and improved cognition. Notably, these peptides demonstrate permeability across the blood−brain barrier, enabling their administration not only through intracranial injection but also via peripheral delivery methods such as intraperitoneal injection or gastric gavage. This property enhances their potential for use in future therapeutic applications.

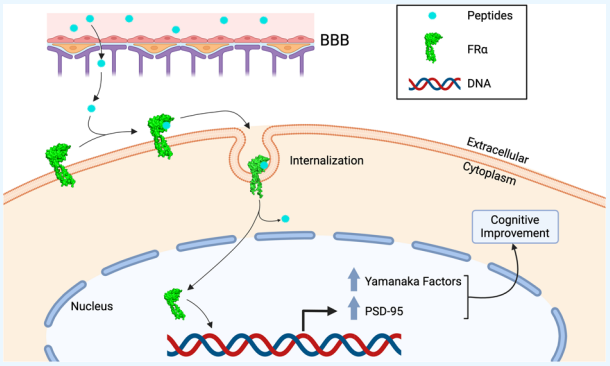

INTRODUCTION

Folic acid or vitamin B9[1] is needed in eukaryotic cells for one-carbon metabolism features like the conversion of homocysteine to methionine, although methionine is the universal methyl donor, folate could also act as a donor through that indirect way.[2] Additionally, folate, with its nine derivates,[3] plays a role in other biological functions like amino acid homeostasis, purines, and thymidylate synthesis or redox defense.[4] Folate and its derivates are transported in cells by (a) the reduced folate carrier, (b) the proton-coupled folate transporter, or (c) the family of folate receptors.[5] Human family of folate receptors include folate receptors α, β, and γ.[6] In this work, we will focus on folate receptor α (FRα), expressed by the FOLR1 gene.

FRα expression is mainly restricted to epithelial and brain cells,[7] although it may appear in tumors present in other tissues (see, for example, ref 8).

Also, the binding of folate to FRα has been analyzed at structural level.[9,10] Upon binding of folate to FRα, the receptor is transported to the cell nucleus, where it acts as transcription factor,[11] facilitating the expression of the so-called Yamanaka factors (YF).[12] Curiously, the expression of YF results in cell reprograming in cells yielding induced pluripotent stem cells[13] from peripheral tissues but not in neuronal cells, where YF only affect at rejuvenation level.[14,15] Indeed, a decrease of folate levels is related to aging[2] and folate supplement is used as a treatment to reduce memory impairment in old people.[16]

However, folate, as previously indicated, is involved in other biological functions, and an increase in folate uptake could result in toxic side effect. Thus, to focus on the interaction of folate-FRα, folate could be replaced by small compounds that bind specifically to FRα. Among those compounds, a small peptide, CTVRTSAEC, has been previously indicated.[17] This peptide could replace folate binding FRα and promoting cell reprogramming.[18]

Now in this work, we tested the effect of the family of FRα binding peptides on mouse cortical cultured neurons. Our results have indicated that folate could be replaced by those peptides for the induction of YF, suggesting a possible future clinical use of them. Moreover, the peptides induce changes in brain cells related to the reorganization of the extracellular matrix, which translate into cognitive improvements even upon intracranial or peripheral delivery in aged wild-type mice. This underscores the clinical potential of these peptides for future treatment strategies for age-related diseases.

Received: November 29, 2024
Revised: January 3, 2025
Accepted: January 6, 2025
Published: March 31, 2025

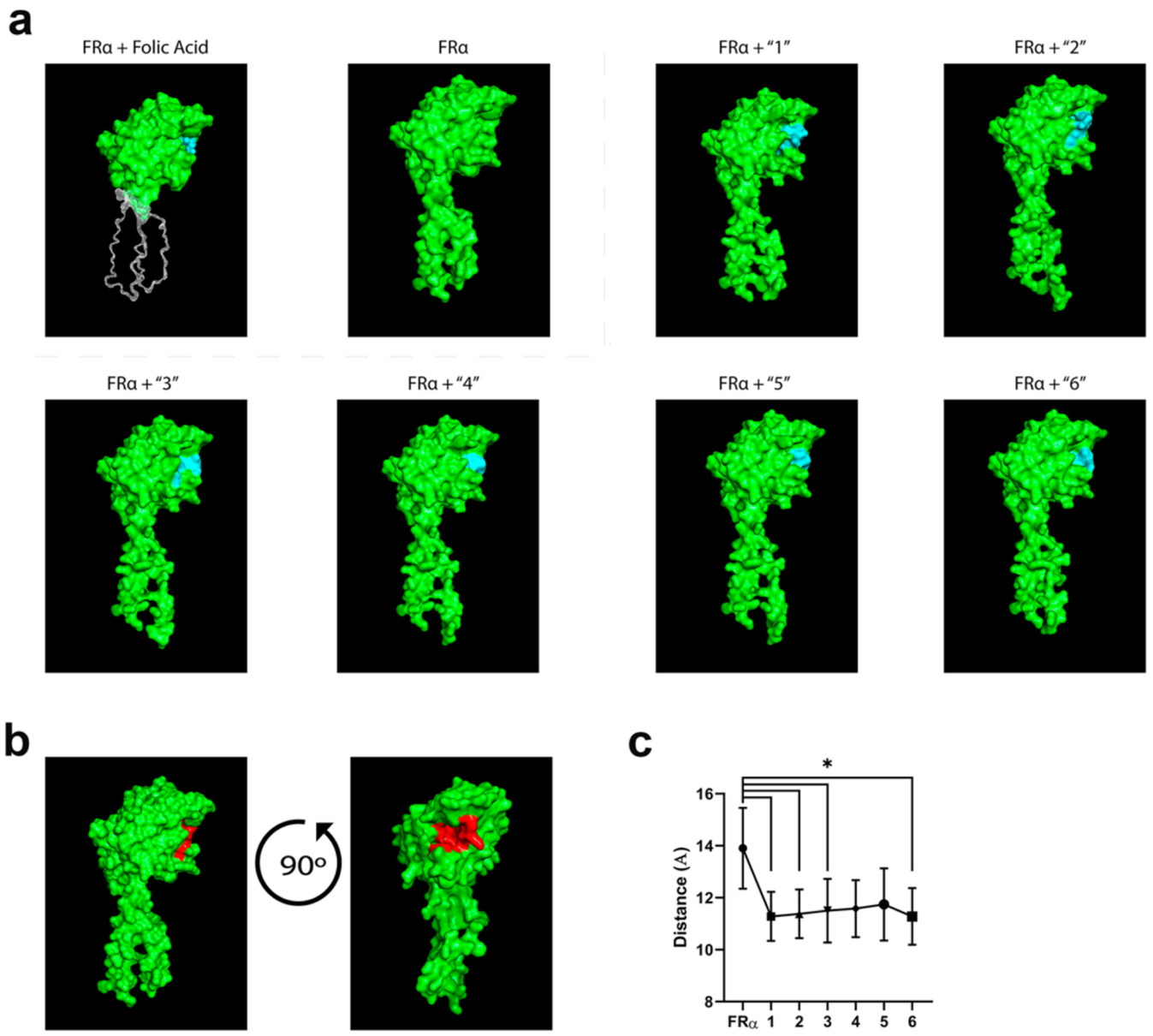

Figure 1. 3D modeling of the binding interaction between FRα and FRα-binding peptides. (a) FRα (green) binding to folic acid extracted from Protein Data Bank (FRα + folic acid), see also refs 9,10. The rest of the molecule is indicated as a sketch based on refs 9,10. Folate receptor modeled by AF2 (FRα)[19] without any ligand (see also ref 10). Binding of folate receptor to peptides (blue), respectively, modeled by AF2, (FRα + "1", FRα + "2", ...). (b) Ligand-binding site (red) representation. (c) Graphical representation of distance between intracellular chains of FRα (see Table 1). One-way ANOVA with Tukey's multiple comparisons test was conducted to study differences in the structure of FRα. Data are presented as mean ± SEM (*$p < 0.05$; **$p < 0.01$; ***$p < 0.001$).

RESULTS

Interaction of Newly Synthesized Small Peptides with FRα. The binding of folate to FRα takes place in the region of FRα comprising residues 80−200.[10,11] On the other hand, folate structure results from the association of 2-amino-4-hydroxy pteridine with *p*-aminobenzoic acid and with glutamic acid. Thus, it has been proposed the interaction of the amino group of folate's pteridine with aspartic 103 of FRα and the interaction of folate's glutamic acid with arginine 158 of FRα.[10]

In a similar fashion, by using AlphaFold modeling (AF2), it can be suggested that the FRα binding peptide CTVRTSAEC[17] could bind to FRα through an ionic interaction involving aspartic acid 103 of the FRα molecule binding to arginine 4 of the peptide, and arginine 158 of the FRα molecule interacting with glutamic acid 8 of the peptide (Figure 1a).

Additionally, the same modeling was used to look for the interaction of FRα with the other five synthesized peptides (Figure 1a). With the use of AF2 protein structure prediction technology, we were able to compare and analyze the binding of different peptides (peptides FR-1-5) to the FOLR1 receptor in comparison to the binding of this receptor to its natural ligand Folic Acid (Figure 1a). The binding of each peptide was found to occur in the same binding pocket used by folic acid (Figure 1b). This binding pocket would be composed of the following amino acids sequence: Y′80, F′82, W′84, D′103, T′104, Y′107, W′124, R′125, W′142, H′157, R′158, G′159, W′160, W′193, S′196, Y′197.

https://doi.org/10.1021/acsomega.4c10849
ACS Omega 2025, 10, 13236−13250

Table 1. Distance between Leucine 9′ and Cysteine 244′ of FRα, Depending on Whether the Ligand Is Unbound to It (FRα) or Bound to FRα-Binding Peptides 1, 2, 3, 4, 5, or 6[a]

	FRα	"1"	"2"	"3"	"4"	"5"	"6"
measure 1	11.5	10.2	10.3	10.4	10.2	10.2	10.2
measure 2	13.5	10.5	10.7	10.6	10.8	10.4	10.2
measure 3	14.0	11.3	11.6	11.2	11.4	11.5	11.3
measure 4	15.0	12.0	12.4	12.3	12.7	12.4	12.1
measure 5	15.5	12.4	12.9	12.4	13.6	13.0	12.6
mean distance	13.9	11.28	11.58	11.38	11.74	11.5	11.28
variance	1.94	0.7096	0.9656	0.6976	1.5504	1.192	0.9496

[a]Each of the measures (measures 1, 2, ...) corresponds to the five highest confidence predictions resolved by AF2. Data represented in Armstrong.

These amino acids will be crucial for the interaction between the receptor and peptides, with amino acid D'103 (aspartic acid at position 103) likely serving as the main anchoring point due to its strong tendency to form salt bridge interactions with basic amino acids[20] such as arginine or lysine, as shown by peptides at position 4 (R-4/K-4). For example, peptides 1 and 2, which have cysteine at their termini, would form a ring structure, leaving the side chains of R and K, respectively, positioned on the outer edge for insertion into the receptor binding pocket. This would create a more efficient overall structure. We identified different potential conformational changes in the intracellular region of the receptor upon external binding of peptides to the FOLR1 receptor. Depending on the binding of different peptides, the distance between the two intracellular domains of FOLR1 varied between each peptide (Figure 1 and Table 1). These distances were analyzed, and results showed significant conformational differences (ordinary one-way ANOVA, $F = 3.072$) owing to peptide binding (Figure 1c). Tukey's multiple comparisons test showed that the "1", "2", and "6" peptides had the lowest mean interdomain distance and the lowest variance (p-value = 0.0254, 0.0347, and 0.0254, respectively) but not mainly differences among peptides were found. Peptides containing both R/K amino acids and the cysteine ring structure, had the shortest distance between domains, followed by those with only one of the key amino acids involved in the bond. Peptides without these amino acids had the longest distance between domains.

After analysis of the different structures formed using the AF2 protein prediction program, slight modifications were seen in the intracellular domain of the receptor. These slight variations turned out to be dependent on the ligand bound. AF2 provides five predictions with the highest confidence. The confidence is quantified by the pLDDT. This value is usually higher for rigid structures or well-studied domains and lower when the program is not confident in predicting that 3D structure. However, recent studies have shown that regions with low pLDDT can be mobile regions within the same protein.[19] These results made a paradigm shift in modeling with the AF2 machine learning system, opening up a range of new opportunities. With this idea, we were able to relate a possible conformational change in the intracellular domain of FOLR1 specific to each ligand. This conformational change is based on the distance between its two parallel chains in the intracellular domain. These distances are significantly reduced in the presence of ligands and further reduced depending on the peptide in question. This reduction in the distance between the intracellular domains together with the idea of being a mobile region could give us clues about how a smaller distance between these regions would increase the signaling capacity of the receptor. This is a key point in understanding how these peptides can regulate the expression of the Yamanaka factors. With this theory, those peptides causing a decrease in the middle distance would give a slight increase in the expression of the Yamanaka factors.

Effect of FRα Binding Peptides on Nuclear Localization of Folate Receptor. We have tested the effect of FRα binding peptides on neuronal cultured cells expressing FRα, such as SK-N-SH neuroblastoma human cells. Upon binding of FRα binding peptides to FRα receptor, an internalization of the folate receptor α in the nucleus was found, as previously described for FR-1.[18] As shown in Figure 2, the FRα binding peptides are also involved in the FRα nuclear internalization (Figure 2a). The presence of nuclear FRα due to the addition of the different peptides was quantified and is shown in Figure 2b.

In addition, it is well known the use of primary cultures of human[21] or mouse[22] cells as models to study different cell mechanisms. Thus, we have used primary cultures of mouse cortical neurons[22,23] to study the effect of FRα binding peptides on FRα nuclear transport and transcription to express specific genes.

Effect of FRα Binding Peptides in Primary Mouse Cortical Neurons. *Transport of FRα to the Nucleus.* To evaluate the internalization of FRα in cortical neurons, we tested the expression of the FRα protein within the nuclear region (labeled with DAPI staining) using confocal microscopy. Figure 2c shows an increase in the reaction with the FRα antibody in the presence of the different FRα binding peptides. The result is quantified in Figure 2d.

Expression of Sox2 and Klf4 upon Addition of FRα Binding Peptides. Previous reports have indicated that FRα-1-binding peptide (or folate) upon binding to FRα favors its transport to the nucleus, where FRα acts as a transcription factor[11] facilitating the expression of Yamanaka Factors (YF).[12,18] There are four YF: Oct4 and Sox2 maintain cell pluripotency and c-Myc and Klf4 regulate cell proliferation.[24] Thus, we study the effect of the FRα binding peptides in the induction of two YF peptides, Sox2 and Klf4. Figure 3 shows that in the presence of the FRα binding peptides, an increase in Sox2 (Figure 3a,b) and Klf4 (Figure 3c,d) protein expression was found.

Expression of Young-Associated Markers in the Presence of FRα Binding Peptides. A previous report[18] described that FRα-1-binding peptide (or folate) may reprogrammate neurons from old brain mice to a younger phenotype, being the expression of GluN2B an example of that partial rejuvenation.[18] GluN2B is a subunit of NMDA receptor, mainly present in young cells[25] that can increase synaptic transmission and cognition,[26] process in which the post-

https://doi.org/10.1021/acsomega.4c10849
ACS Omega 2025, 10, 13236−13250

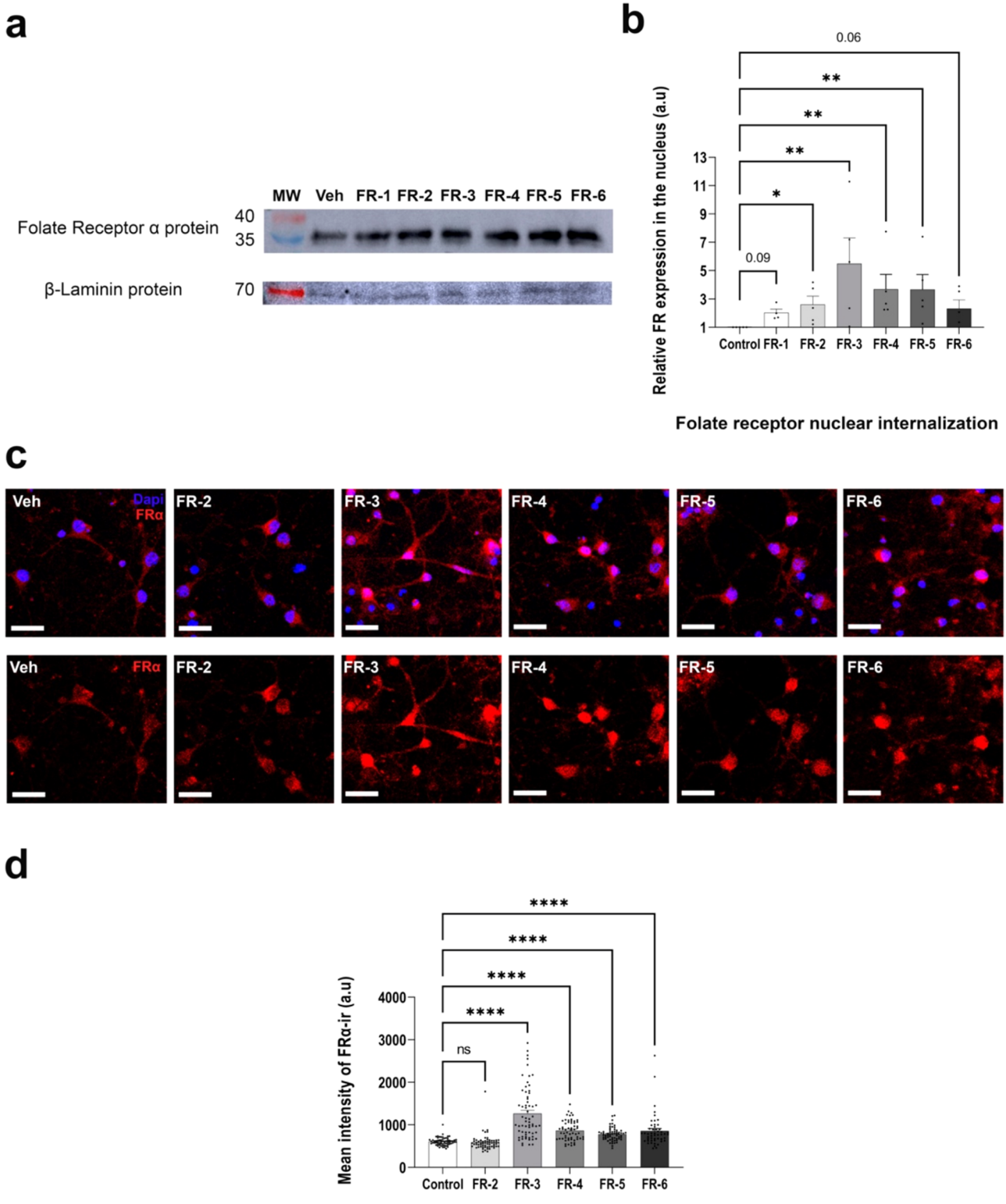

Figure 2. Effect of FRα binding peptides on the nuclear internalization of FRα. (a) Representative examples of a Western blot of SK-N-SH human cellular cultures using an FRα antibody and β-Laminin as a loading control. (b) Quantification of nuclear FRα protein expression following a 30 min incubation with either a vehicle solution or different folate receptor FRα-binding peptides. The addition of peptides increases FRα protein expression in cells compared to the vehicle (Kruskal–Wallis value = 14.22, $p < 0.0273$, df = 7). The intensity of the FRα immunoreactivity signal was quantified relative to the β-Laminin signal detected in the same experiment. (c) Representative confocal images of neocortical neurons from primary cultures showing FRα (red) immunofluorescence expression after treatment with vehicle or different FRα-binding peptides (FR-2-6). In blue is shown DAPI nuclear marker. (d) Bar graphs showing the mean intensity from FRα immunofluorescence signal. The value of each neuron analyzed (represented by black dots) is displayed, with data collected from a total of 359 neurons in panel (d). Treatment with different FR α-binding peptides induced a significant increase in neuronal FRα nuclear expression (Kruskal–Wallis value = 57.92, $p < 0.0001$, df = 5). Data are presented as mean ± SEM (*$p < 0.05$; **$p < 0.01$; ***$p < 0.001$). Scale bars, 25 μm (c).

https://doi.org/10.1021/acsomega.4c10849
ACS Omega 2025, 10, 13236−13250

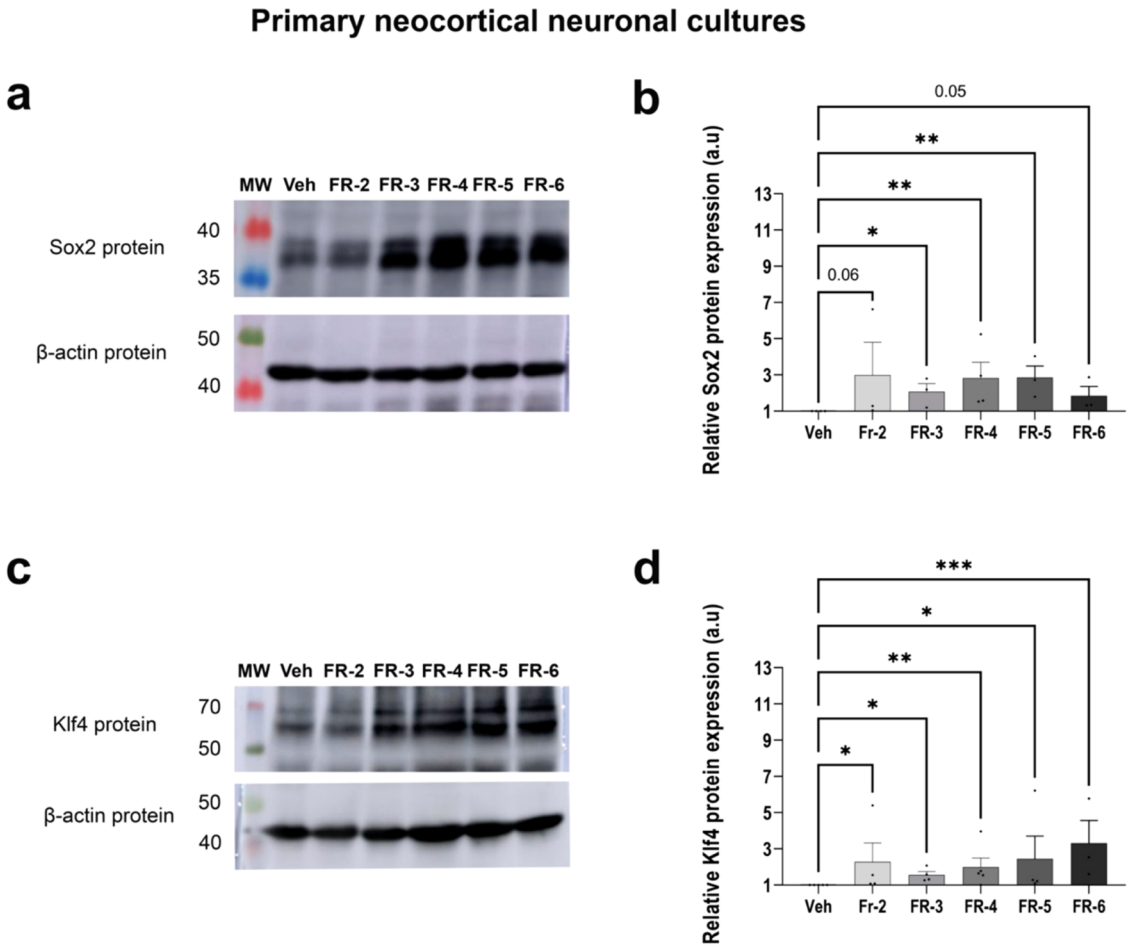

Figure 3. Effect of FRα binding peptides on neuronal Sox2 and Klf4 protein expression. (a) Representative examples of a Western blot of primary neocortical neuronal cultures from wild-type mice using a Sox2 antibody and β-actin as a loading control. (b) Quantification of Sox2 protein expression following a 30 min incubation with either a vehicle solution or different folate receptor FRα-binding peptides. The addition of peptides increases Sox2 protein expression in neurons compared to the vehicle (Kruskal–Wallis value = 10.57, $p < 0.06$, df = 5). The intensity of the Sox2 immunoreactivity signal was quantified relative to the β-actin signal detected in the same experiment. Data are presented as mean ± SEM (*$p <$ 0.05; **$p < 0.01$). (c) Representative examples of a Western blot of primary neocortical neuronal cultures from wild-type mice using a Klf4 antibody and β-actin as a loading control. (d) Quantification of Klf4 protein expression following a 30 min incubation with either a vehicle solution or different FRα-binding peptides. The addition of peptides increases Klf4 protein expression in neurons compared to the vehicle (Kruskal–Wallis value = 13.69, $p < 0.0177$, df = 5). The intensity of the Klf4 immunoreactivity signal was quantified relative to the β-actin signal detected in the same experiment. Data are presented as mean ± SEM (*$p < 0.05$; **$p < 0.01$; ***$p < 0.001$).

synaptic protein PSD-95 may play a role by its direct binding to GluN2B.[27] Thus, we studied the presence of PSD95 in cultured mouse cortical neurons. Figure 4a shows that FRα binding peptides increase the level of the presence of PSD95 in cortical neurons. A quantification of the results of Figure 4a is indicated in Figure 4b.

Other Markers for FRα Binding Peptides In Vivo Effect. In a previous work, it was shown that intracranial injection of folate or a FRα binding peptide[10] in aged wild-type mice results in the change in the extracellular matrix organization known as perineuronal nets (PNNs) present at dentate gyrus and comprising proteoglycans like neurocan, brevican, aggrecan, phosphocan and versican. Aging is associated with an increase in PNN at DG[18] that could be reduced by the presence of folate or a FRα binding peptide (FR-1).[18] Thus, the reduction of PNNs could be a good marker for the rejuvenation effects of the FRα binding peptides.

Considering the promising results that these newly synthesized peptides had on in vitro neurons, we wanted to test their potential in vivo effects. We then started studying the first of the newly synthesized peptides (FR-2). We have first replicated the treatment protocol previously carried out with FR-1,[18] injecting the peptide intrahippocampally to verify if it could produce a more potent effect in terms of changes in the extracellular matrix (Figure 5a). The results showed that FR-2 indeed had a very significant effect on the hippocampus, reducing the density of perineuronal nets in the injection area (Figure 5b). Next, we wanted to better understand the delivery possibilities of these new peptides. Therefore, we examined their ability to efficiently cross the blood–brain barrier and produce significant effects on the nervous system as well.

Intraperitoneal Peptide Delivery and Its Effects on the Brain. Looking for a possible human clinical use of these FRα binding peptides, we tested the intraperitoneal delivery of these peptides, searching for a further brain effect.

Figure 5c–e shows that intraperitoneal delivery of FRα binding peptide 2 results in similar brain marker (PNNs) changes to those previously observed for intracranial injection of the same peptide (see Figure 5a,b and also ref 18). In the

https://doi.org/10.1021/acsomega.4c10849
ACS Omega 2025, 10, 13236–13250

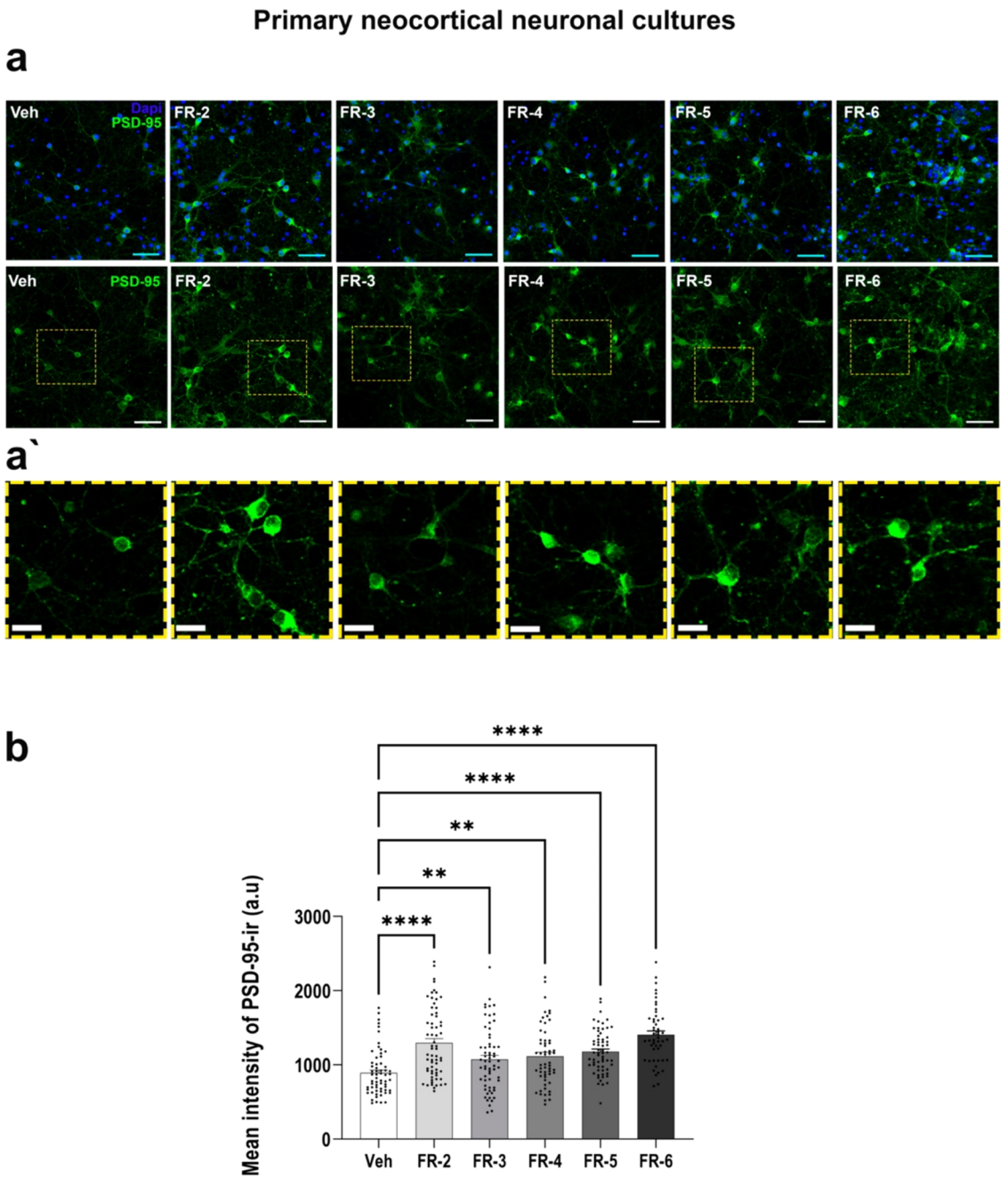

Figure 4. Effect of folate receptor (FR) α-binding peptides on the expression of PSD-95 postsynaptic neuronal protein in neocortical neurons. (a) Representative confocal images of neurons showing PSD-95 (green) immunofluorescence expression after treatment with vehicle or different FRα-binding peptides (FR-2-6). In blue is shown DAPI nuclear marker. (a′) A magnified view of the square-segmented region highlighted in (a) is displayed. (b) Bar graphs showing the mean intensity from PSD-95 immunofluorescence signal. The value of each neuron analyzed (represented by black dots) is displayed, with data collected from a total of 359 neurons in panel (b). Treatment with different FR α-binding peptides induced a significant increase in neuronal PSD-95 expression (Kruskal–Wallis value = 151.6, $p < 0.0001$, df = 5). Data are presented as mean ± SEM (*$p <$ 0.05; **$p < 0.01$; ***$p < 0.001$). Scale bars, 50 μm (a), 20 μm (a′).

intraperitoneal treatment, we found changes not only at hippocampal levels (Figure 5e) but also on the somatosensory neocortex, where a significant decrease of PNN density was found (Figure 5d).

Effect of FRα-2 Binding Peptide Administration via Intracranial Injection or Peripheral Delivery (Intraperitoneal Injection or Intragastric Inoculation) on Cognition. Moreover, similar effects in these aged wild-type mice were found using either delivery type at the level of cognitive improvement (Figure 6). In both cases, there was a notable improvement in new object recognition memory, particularly in the long term but also in short-term spatial memory. In the case of intraperitoneal injection, we observed a significant improvement in stress and anxiety levels in the aged mice. These results confirmed that intraperitoneal injection of the peptide was able to reach the nervous system and induce positive functional changes in cognition.

A possible explanation (see Table 2) is the high probability calculated for these FRα binding peptide to cross BBB, by following the model of Chen et al.[28]

https://doi.org/10.1021/acsomega.4c10849
ACS Omega 2025, 10, 13236−13250

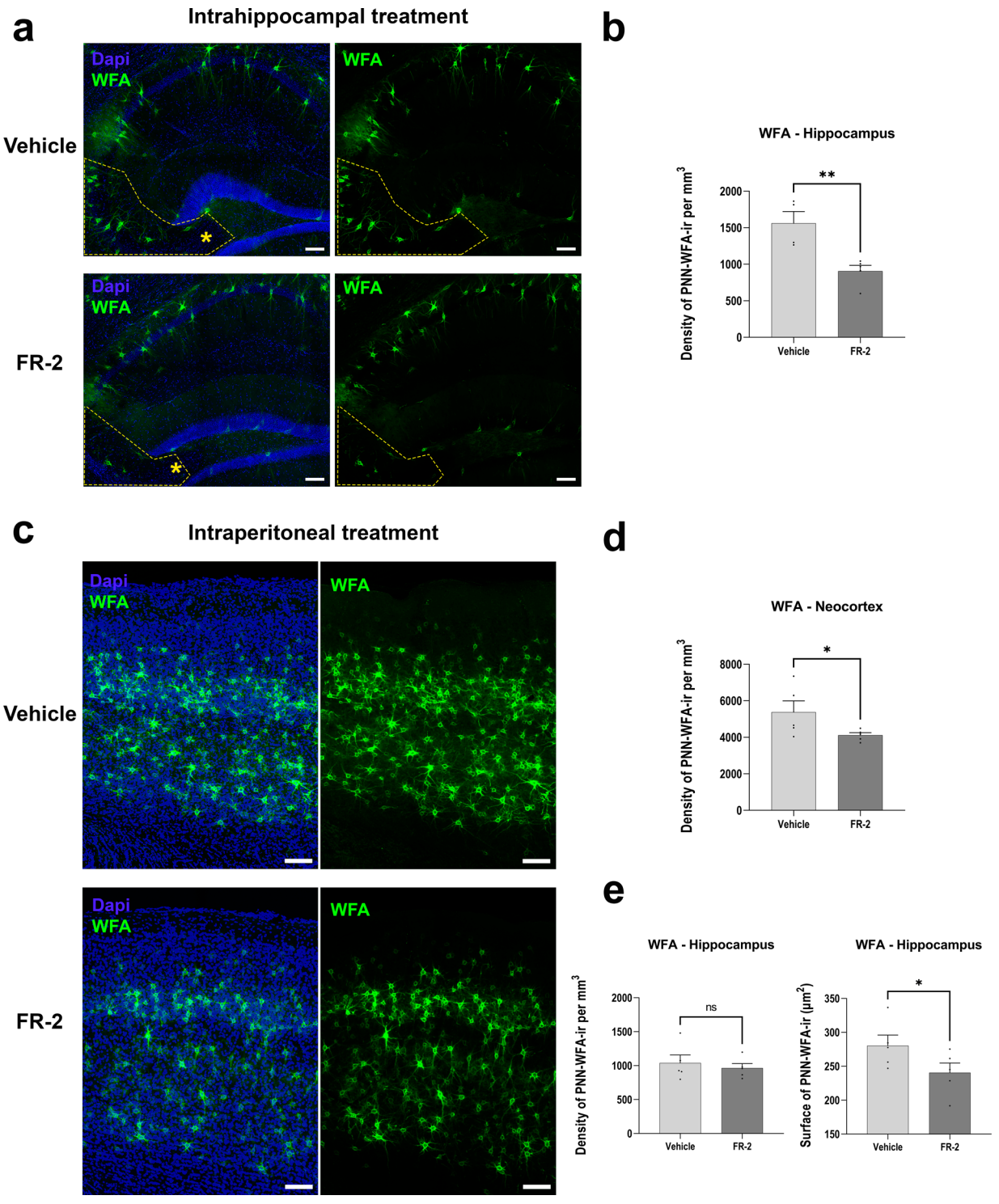

Figure 5. Immunofluorescence results for Wisteria Floribunda (WFA) expression after intrahippocampal and intraperitoneal vehicle or FR-2 treatment. (a) Representative microphotographs of immunoreactivity obtained for WFA protein expression (green) in the hippocampus from vehicle-treated and FR-2-treated mice. The segmented area corresponds to the CA3 region, where the analysis was performed. The yellow asterisk represents the area where the selected treatment was microinjected. Scale bar shown in (a) indicates 100 μm. (b) Graphical representation of the mean ± SEM of the perineuronal net (PNN) WFA-immunoreactive cell density per mm^3 in the total volume of the CA3 region. Mice intrahippocampally treated with the FR-2 peptide showed a significant reduction of PNN density (t = 3.526; df = 7). (c) Representative microphotographs of immunoreactivity obtained for WFA protein expression (in green) in the somatosensory neocortex from intraperitoneal-treated mice. Scale bar shown in (c) indicates 200 μm. (d) Graphical representation of the mean ± SEM of the perineuronal net (PNN) WFA-immunoreactive cell density per mm^3 in the total volume of somatosensory neocortex. Mice intraperitoneally treated with the FR-2 peptide showed a significant reduction of PNN density (t = 1.977; df = 8). (e) Graphical representation of the mean ± SEM of the perineuronal net (PNN) WFA-immunoreactive cell density per mm^3 in the total volume of the CA3 hippocampal region (left panel) and the mean surface area of those PNN WFA-immunoreactive units. Mice intraperitoneally treated with the FR-2 peptide showed in the hippocampus a significant reduction of PNN surface area (t = 1.874; df = 8). *p < 0.05, **p < 0.01.

https://doi.org/10.1021/acsomega.4c10849
ACS Omega 2025, 10, 13236−13250

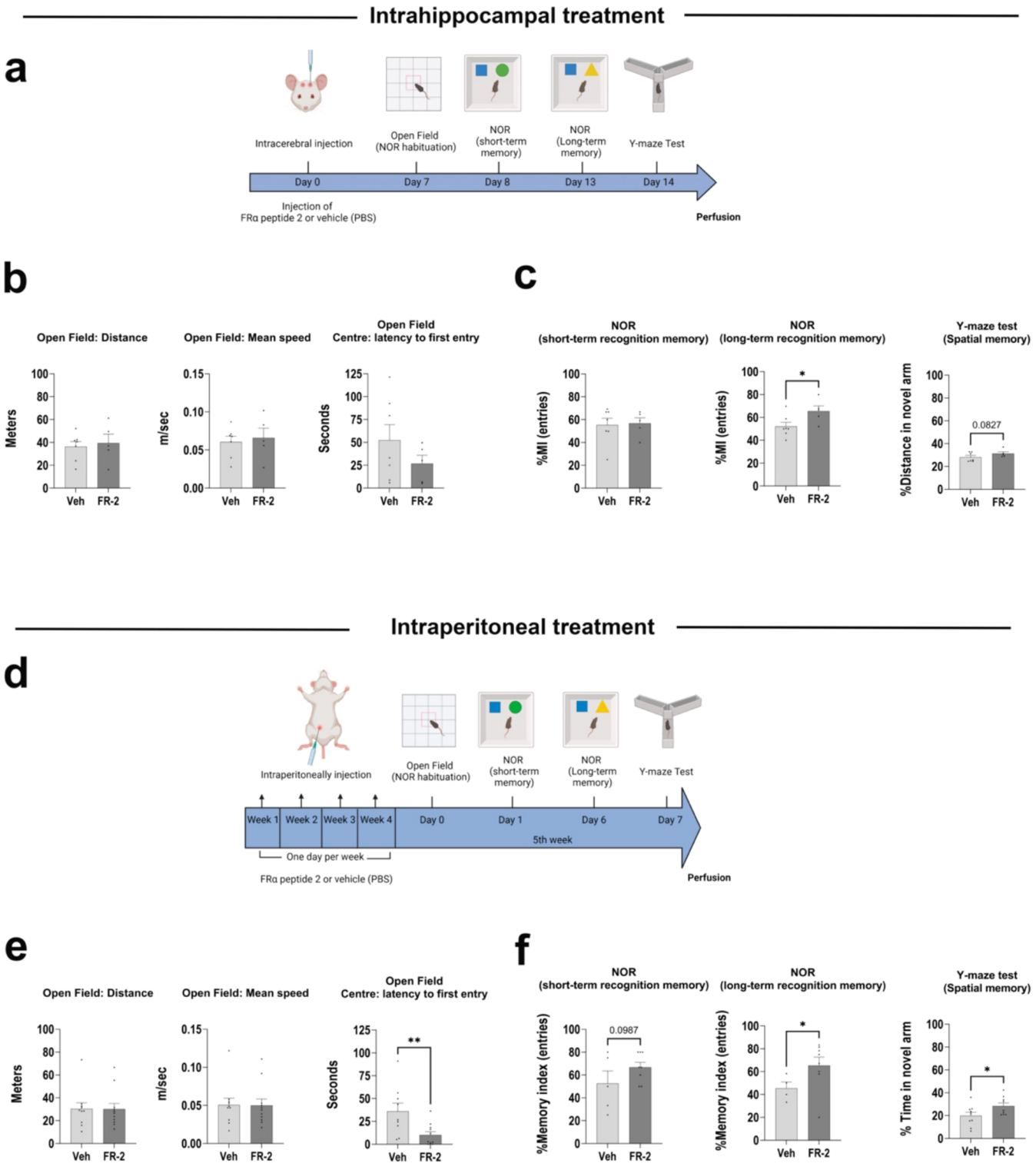

Figure 6. Effect of intrahippocampal FR-2 peptide treatment on cognition. (a) Graphical scheme of the protocol followed for the behavioral study of animals subjected to intrahippocampal treatment with the peptide or vehicle solution is shown. (b) Bar graphs show some of the main data from the open field test in mice treated with FRα-binding peptide FR-2: total distance traveled, average speed of movement, and latency to first entry to the center area of open field. No changes were found after FRα-binding peptide treatment in anxiety-depression-like behavior (t = 1.166, df = 10 for latency to first enter to the center area), nor in general motor activity (t = 0.3545, df = 10 for total distance traveled and 0.3522, df = 10 speed average). (c) Bar graphs show the results from two memory tests: the novel object recognition (NOR) for short-(2 h) and long-term recognition memory (5 days) and the Y-maze test for spatial memory. Mice treated with the peptide showed a significant improvement in memory retention 5 days after the first training session, as shown by memory index of novel object recognition test (Mann−Whitney test, p = 0.0364). Treatment with FRα-binding peptide induced a strong tendency toward a significant effect on spatial memory performance, as shown by the percentage of time spent in the novel arm (t = 1.496, df = 10). Graphs displaying mean ± SEM of both the vehicle-treated group and the peptide-treated group are shown. All data were analyzed by Student's t test or Mann−Whitney test depending on whether the data met the requirements for normality. *p < 0.05. Effect of Intraperitoneal FR-2 Peptide Treatment on Cognition. (d) Graphical scheme of the protocol followed for the behavioral study of

https://doi.org/10.1021/acsomega.4c10849
ACS Omega 2025, 10, 13236−13250

Figure 6. continued

animals subjected to intraperitoneal treatment with the peptide or vehicle solution is shown. (e) Bar graphs show some of the main data from the open field test in mice treated with FRα-binding peptide FR-2: total distance traveled, average speed of movement, and latency to first entry to the center area of open field. No changes were found after FRα-binding peptide treatment in general motor activity (t = 0.03481, df = 19 for total distance traveled and 0.04168, df = 19 speed average), but there was an improvement in stress and anxiety levels (t = 2.834, df = 18 for latency to first enter to the center area). (f) Bar graphs show the results from two memory tests: the novel object recognition (NOR) for short (2 h)- and long-term recognition memory (5 days) and the Y-maze test for spatial memory. Mice treated with the peptide showed a significant improvement in object recognition memory, either 2 h (strong tendency, t = 1.372, df = 11) and 5 days (Mann−Whitney test, p = 0.0364) after the first training session. Treatment with FRα-binding peptide induced also significant effect on spatial memory performance as shown by the percentage of time spent in novel arm (t = 2.077, df = 16). Graphs displaying mean ± SEM of both the vehicle-treated group and the peptide-treated group are shown. All data were analyzed by Student's t test or Mann−Whitney test depending on whether the data met the requirements for normality. *p < 0.05.

Table 2. Key Biochemical Data of Newly Synthesized Small Peptides, Including Amino Acid Composition, Molecular Weight (g/mol), HPLC Purity (%), Probability to Cross the Blood−Brain Barrier According to BBP Predict Software (All Are Predicted to Be Blood−Brain Barrier Peptides), and a Schematic Representation of the Molecular Structure

Name	Composition	MW (g/mol)	Purity	BBP Predict	Molecular structure
FRα-binding Peptide 1	CTVRTSAEC	969.09	95.39%	**69%**	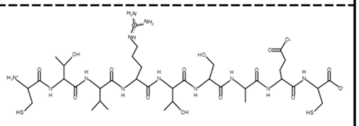
FRα-binding Peptide 2	CTVKSTADC	927.05	95.16%	**65%**	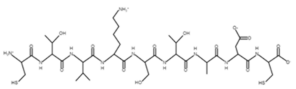
FRα-binding Peptide 3	TVRTSAE	762.8	95.03%	**65%**	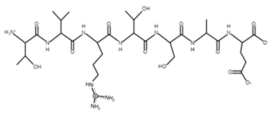
FRα-binding Peptide 4	TVKSTAD	720.76	95.23%	**59%**	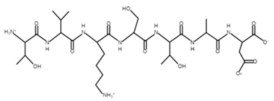
FRα-binding Peptide 5	SAKSTVD	706.74	95.85%	**62%**	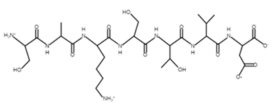
FRα-binding Peptide 6	RTSAE	562.57	95.05%	**70%**	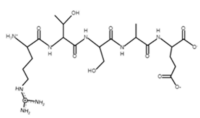

Even intragastric inoculation of the peptide led to cognitive effects, significantly improving the spatial memory of aged and treated mice. However, no significant behavioral effects were observed in terms of mobility, stress, or anxiety levels (Figure S1).

DISCUSSION

In this work, we have found that several peptides related to the previously indicated CTVRTSAEC,[17] from now named as FR-1, are able to bind FRα at the same localization as folic acid, minimizing the potential toxic side effects of folic acid, and inducing the transcription of YF like Sox2 or Klf4.[12,18]

In the interaction of FRα binding peptides with FRα, different types of bonds take place: ionic bonds between glutamatic/aspartic residues with arginine/lysine amino acids or hydrogen bands between tyrosine (−OH) and serine/tyrosine (−OH).

The analysis using the AF2 protein prediction software revealed slight ligand-dependent modifications in the intracellular domain of the receptor. Notably, these changes were

https://doi.org/10.1021/acsomega.4c10849
ACS Omega 2025, 10, 13236−13250

linked to a decrease in the distance between parallel chains within the intracellular domain in the presence of ligands. AF2's pLDDT scores helped us to consider the hypothesis that conformational changes in mobile regions, like the intracellular domain of FRα, could enhance receptor signaling by reducing the distance between domains.

After gaining a better understanding of the mechanism of action of these new peptides through their interaction with the folate receptor α, we aimed to study the sequences of these peptides more closely and explore possible homologies with existing sequences. By looking at the *Homo sapiens* (Taxon ID:9606) protein database,[29] we have tested if the sequence of any of those peptides could be present in any reported human protein. Only FRα binding peptide 3 (TVRTSAE) sequence was found to be present in Shcbp1 protein.[30] Shcbp1 is a protein that interacts with the adapter protein p52 ShcA, a factor involved in T cell activation.[31] Also, Shcbp1 is involved in several signaling pathways,[32] mainly through its interaction with Shc protein as well as in the regulation/dysregulation of several processes,[32] including neurodegenerative disorders.[33] The interaction of Shcbp1 with Shc proteins occurs through an acid region of Shcbp1, present at its NH_2 half of the protein, which binds to the SH_2 domain of Shc protein.[30,31] However, the sequence TVRTSAE (present in the FRα binding peptide 3) is located in the CO_2H half of the Shabp1 molecule.[31] Further work will be needed to know whether there is a possible relation, or not, between FRα and Shcbp1 protein.

Regarding the effects of these new peptides at the cellular and organismal levels, we have found significant and promising results. The administration of folate-receptor-binding peptides to cortical neurons significantly promotes the transport of FRα to the cell nucleus, where it functions as a transcription factor, enhancing the expression of Yamanaka factors such as Sox2 and Klf4. The expression of Yamanaka factors in the brain, and specifically in neurons, has been shown to reverse different aging-associated phenotypes, including the increase of synaptic receptors or the neuronal activity of circuits associated with memory, improving memory functioning.[15,18] One of these synaptic proteins was GluN2B, a subunit of NMDA receptors, mainly present in young brain cells[15,18] and linked to the postsynaptic protein PSD95.[27] Its increased expression results in improved cognition in old animals. Indeed, PSD95 is a major synaptic protein involved in aging.[34] The expression of this protein has indeed been found to be significantly reduced with aging in numerous studies, both in genetic models of premature aging[35] and with physiological aging,[36] typically accompanied by a decline in memory processing. Considering these previous data, the increase in PSD95 expression in mature cortical neurons found in this study after treatment with FR-2 suggests a rejuvenating effect at the cellular level by these peptides by enhancing neuronal plasticity.

Furthermore, the expression of Yamanaka factors in neurons from in vivo mouse models has been also shown to reverse other age-associated phenotype such as the increased presence of organized extracellular matrix in the so-called perineuronal nets.[37]

Various studies have found that during partial reprogramming induced by the overexpression of Yamanaka factors, which leads to a cellular rejuvenation process both peripherally and in the central nervous system, there are systematic changes in the extracellular matrix.[18,38] Our previous studies have determined that such partial reprogramming,[18] led to a reduction in the extracellular matrix and the perineuronal nets they form. The in vivo results obtained in this work similarly reproduce those findings reached by transgenic overexpression of YF, reducing the perineuronal net density after the intrahippocampal application in aged mice of one of these peptides, FR-2. This protocol has also reproduced some of the effects previously observed with FR-1,[17] resulting in cognitive improvement. In that improvement, there is, as indicated, a decrease of PNNs, reverting that aging hallmark.[39]

However, the major milestone achieved in this study is the potential reach of the effects of these peptides through peripheral administration. The intraperitoneal injection of this same peptide (FR-2) in aged mice, once per week for a full month, resulted in the same type of changes seen previously regarding the extracellular matrix of the cerebral cortex along with an improvement in object recognition and spatial memory. Additionally, an improvement in spatial memory was observed when the same peptide was administered via gastric gavage in aged mice. This ability to exert a cognitive effect when administered peripherally through different types of inoculations would confirm the theoretical potential observed regarding the permeability of these peptides in the blood–brain barrier like FRα peptide 1.[28]

In summary, we have indicated the effect of a family of FRα binding peptides to activate the expression of some YF in cultures of cortical neurons or in vivo, by intrahippocampal, intraperitoneal, or intragastric injections, resulting in an increase of cognitive improvement.

METHODS

Synthesis of Different FRα-Binding Peptides. To mimic the cognitive results produced by intrahippocampal injection of folate, we have characterized different FRα-binding peptides with the following sequence: cys–thr–val–arg–thr–ser–ala–glu–cys (CTVRTSAEC), thr–val–arg–thr–ser–ala–glu (TVRTSAE), arg–thr–ser–ala–glu (RTSAE), thr–val–lys–ser–thr–ala–asp (TVKSTAD), cys–thr–val–lys–ser–thr–ala–asp–cys (CTVKSTADC), and ser–ala–lys–ser–thr–val–asp (SAKSTVD) (Figure S1). These peptides were prepared by the company Proteogenix (Schiltigheim, France) and in Table 1 their biochemical properties.

AlphaFold Modeling. The amino acid sequence of FOLR1 was extracted from its respective entry in the UniProtKB database (P35846). A user-friendly interface for accessing AlphaFold2 (AF2) has recently been made available through notebooks. We used the ColabFold notebook, whose structure prediction is powered by AF2 combined with RoseTTAFold, a software tool that uses deep learning to quickly and accurately predict protein structures [1], and a fast multiple sequence alignment generation stage using another software which search and cluster huge sequence sets (MMseqs2).[40] Using the AF2 program, the FASTA format of each sequence serves as input and the program predicts five structures for each sequence in a single execution. Each ligand–receptor binding structure prediction was downloaded from ColabFold with the exception of the linkage between FOLR1 and Folic Acid, which was downloaded from the Protein Data Bank (PDB) obtained through X-ray crystallography data.[41] This last interaction prediction barely showed the intracellular region due to the technical limitations of the results obtained through X-ray crystallography. Every structure was analyzed, visualized, and colored with the PyMOL Molecular Graphics System (Version 2.0 Schrödinger, LLC). Based on the five structures predicted by AF2, we were able to

https://doi.org/10.1021/acsomega.4c10849
ACS Omega 2025, 10, 13236−13250

find slight structural variations in the conformations of the FOLR1 receptor. These variations were found among the most likely predicted structures contributed by the same peptide, between different peptides, and when compared against the folate receptor without a ligand. To study these variations in depth, the Pymol measurement program was used, in which two random amino acids were chosen (Leucine 9′ and Cysteine 244′), each one belonging to one of the two intracellular domains of the FOLR1 structure. We then analyzed the distance between both amino acids in the three-dimensional configuration of the folate receptor in each of the cases studied, namely, with the peptide binding (in each of its 5 most probable configurations), and compared it with the distance between both amino acids in the receptor without bound ligand.

Nuclear Fractionation of Cultured Human Cells and Western Blotting. To study the efficiency of different peptides in translocating the FRα receptor into the nucleus, as well as inducing the expression of different Yamanaka factors such as Sox2 or Klf4, we used SK-N-SH human neuroblastoma cell line.[42] The method to fractionate the cell nucleus has been reported previously,[18] and the presence of FRα-binding peptide in the nuclear fraction was demonstrated by Western blot analysis using the antibody against FRα1-binding peptide (Thermo Fisher, ref: PA5-101588). SK-N-SH cells were treated with different FRα-binding peptides (1 mM), or Dulbecco's Modified Eagle Medium (DMEM) for 30 min at 37 °C. Total cell lysate or nuclear fraction was obtained as previously reported.[43] Whole cell lysate or cell nuclear pellets of each experiment were then quantified by the BCA protein assay. Samples were separated on 10% SDS-PAGE and electrophoretically transferred to a nitrocellulose membrane (Schleicher & Schuell GmbH). The membrane was blocked by incubation with 5% semifat dried milk in PBS and 0.1% Tween 20 (PBS), followed by a 1 h incubation at room temperature with the primary antibody in PBSM. The following primary antibody dilutions were used: antifolate receptor α 1 (1/300; Thermo Fisher, ref: PA5-101588) for nuclear fraction. In all cases, β-Laminin (Santa Cruz SC-377000, diluted 1/1000) was used as loading control. After three washes, the membrane was incubated with a horseradish peroxidase-antirabbit Ig conjugate (DAKO), followed by several washes in PBS-Tween 20. The membrane was then incubated for 1 min in Western Lightning reagents (PerkinElmer Life Sciences). Blots were quantified using the EPSON Perfection 1660 scanner and the ImageJ software.

Primary Neuron Culture and Treatments. Cortical neuronal cultures were obtained from embryonic day E18 C57JBL mouse embryos. After removing meninges, entire cortices were first incubated with trypsin 10× (Sigma) and DNAase (Roche) in HBSS for 15 min at 37 °C and then mechanically dissociated using a Pasteur pipet. The reaction was halted using medium plating (HS medium, glucose 20%, 50 mg/mL gentamicin, and MEM) followed by centrifugation at 800 rpm for 10 min. Subsequently, the pellet was reconstituted in plating medium and placed at a density of 106 cells/cm^2 on glass coverslips coated with poly-D-lysine (100 μg/mL; Invitrogen) or in 35 mm dishes in the incubator at 37 °C and 5% CO_2. After 3 h, the medium was replaced with Neurobasal (NB) culture medium complemented with 2% B27, 500 mM GlutaMAX supplement (Invitrogen), and antibiotics (gentamicin 50 mg/mL). The following day AraC was introduced into the medium at a concentration of 5 μM and the culture medium was refreshed on day 7, wherein it is substituted with freshly prepared NB+B27 medium. Half of the culture medium was exchanged each 5−6 days and cells were used at DIV 14. On the 14 DIV, PBS (vehicle solution) or the peptide was added to the medium at a concentration of 5 mg/mL for 30 min. After this period, the cells were washed with PBS, dissociated, frozen, or fixed on coverslips with 4% PFA.

Primary Neuron Western Blotting. After neuron homogenization, samples were separated on 10% SDS-PAGE and electrophoretically transferred to a nitrocellulose membrane (Schleicher & Schuell GmbH). The membrane was blocked by incubation with 5% semifat dried milk in PBS and 0.1% Tween 20 (PBS), followed by 1 h incubation at room temperature with the primary antibody in PBSM. The following primary antibody dilutions were used: anti-Klf4 (1/1000; R&D System, ref: AF3158) and anti-Sox2 (1/1000; R&D Systems, ref: AF2018) for total cell lysate. β-actin (1/5000; SIGMA, ref: T4026) was used as loading control. After three washes, the membrane was incubated with a horseradish peroxidase-antigoat Ig conjugate (DAKO), followed by several washes in PBS-Tween 20. The membrane was then incubated for 1 min in Western Lightning reagents (PerkinElmer Life Sciences). Blots were quantified using the EPSON Perfection 1660 scanner and ImageJ software.

Primary Neuron Immunofluorescence. For immunofluorescence studies, cells were fixed with 4% formaldehyde. Subsequently, the fixed cells were permeabilized with 0.1% Triton X-100 and 1 M glycine for 30 min. After fixation, the coverslips were blocked with 1% bovine serum albumin for 30 min and subsequently incubated with primary antibodies (antifolate receptor α 1, 1/300, Thermo Fisher, ref: PA5-101588; anti-PSD95, 1/500 Synaptic Systems, ref: 124014) in PBS containing 1% bovine serum albumin for 1 h. Coverslips were rinsed three times with PBS and incubated for 45 min with Alexa 488-conjugated antiguinea pig (diluted 1:500; Thermo Fisher) and Alexa 594-conjugated antirabbit (diluted 1:400; Thermo Fisher). All of the coverslips were finally counterstained for 3 min with 4′,6-diamidine-2′-phenylindole dihydrochloride (DAPI; 1:1000, Calbiochem-EMD Darmstadt, Germany). After being washed with PBS, the coverslips were mounted with Fluorosave (Calbiochem, San Diego, CA).

Ethics Statements. Animals were housed in accordance with European Community Guidelines (directive 86/609/EEC) and handled following European and local animal care protocols. The animal experiments were approved by the CBMSO Ethics Committee (AECC-CBMSO-13/172) and the National Ethics Committee (PROEX 102.0/21). All of the methods were performed in accordance with the relevant guidelines and regulations. The study is reported in accordance with ARRIVE guidelines (https://arriveguidelines.org).

Animals. Animals were housed in a specific pathogen-free facility under standard laboratory conditions. They were housed 4−5 per cage with food and water available ad libitum and maintained in a temperature-controlled environment on a 12/12 h light/dark cycle with light onset at 8 a.m. A total of 44 C57BL/6 wild-type male (XY) and female (XX) mice were bred in the animal facility at the CBM.

Experimental In Vivo Designs. To study the in vivo effects of this new family of synthetic peptides, we tested FRα-binding peptide 2 (FR-2; TVRTSAE) was tested. This peptide was administered intracerebrally, similar to what was done previously with FR-1.[17] According to a software tool predictor created by Chen et al.[28] (BBP predict), this peptide has the

https://doi.org/10.1021/acsomega.4c10849
ACS Omega 2025, 10, 13236−13250

potential ability to cross the blood−brain barrier with a probability of 65%. Taking advantage of this capacity, the peptide was also injected intraperitoneally to verify its ability to reach the brain through peripheral administration. In both experiments, 1 week after the injections, the mice were assessed using behavioral (open field trial) and memory tests (novel object recognition and Y maze test) to determine the potential functional effects of the peptide on the central nervous system. Two weeks after surgery, the mice were perfused immediately after completing the Y maze test.

Stereotaxic Surgery and Intrahippocampal Microinjection. A group of 13 wild-type C57JBL 26-month-old mice were randomly injected in the hilus region of both brain hemispheres (2 μL in each one) with vehicle (phosphate-buffered saline, PBS), or synthetic FRα-binding peptide 2 (5 mg/mL, diluted in PBS; Abyntec; amino acid sequence: CTVKSTADC; M.W., 927 Da).

After anesthesia with isoflurane, the mice were secured in a stereotaxic frame (Kopf). Holes were drilled bilaterally in the skull at the injection sites (one per hemisphere) using a microdrill with a 0.5 mm bit. The following stereotaxic coordinates were used for intrahippocampal injections (from bregma): anterior−posterior −2.0; lateral 1.4; and dorsoventral −2.2. A 33-gauge needle Hamilton syringe coupled to a syringe pump controller mounted on the stereotaxic frame was used to inject 2 μL of vehicle or metabolites at each site. Injections were given at 0.25 μL/min, and after completing the inoculation of the entire solution volume, a 3 min wait was observed before removing the needle from the injection site. Prior to completely removing the needle from the brain tissue, another 3 min pause was implemented halfway through in order to minimize potential damage. After the injections, the skin was sutured, and buprenorphine (Sigma) was administered subcutaneously. The animals were allowed to recover for 1 h on a heating pad before being returned to the cage. The animals were treated with ibuprofen (Dalsy in drinking water) for the following 5 days. They remained in the cage for an additional week before the start of behavior tests and were sacrificed 2 weeks after surgery.

Intraperitoneally Delivery. For a more realistic clinical approach, we intraperitoneally injected the same synthetic FRα-binding peptide into another group of 21 wild-type C57JBL mice that were 19 months old. The animals were injected once per week, with two injections of 150 μL spaced an hour and a half apart on the same day, for the duration of a whole month. These injections consisted of either the vehicle (phosphate-buffered saline, PBS) or the peptide (5 mg/mL, diluted in PBS).

Gastric Gavage Delivery. Finally, to evaluate the potential of a more accessible treatment, such as oral administration, we studied behavioral effects in aged mice treated via gastric gavage with the FRα-binding peptide 2, in order to economize on peptide usage. A group of 10 wild-type C57JBL mice, averaging 18 months of age, was used, and the same protocol previously applied for intraperitoneal delivery was followed. A weekly administration (always on the same day for all mice) of 300 μL was performed via gastric gavage at a concentration of 5 mg/mL of the peptide diluted in PBS, or PBS alone for the control group. Behavioral tests started the day after the last administration (Figure S1).

Animal Sacrifice and Tissue Processing. The mice were anesthetized with an intraperitoneal pentobarbital injection (Dolethal, 60 mg/kg body weight) and transcardially perfused with saline. Brains were separated into two hemispheres. One was removed and fixed in 4% paraformaldehyde in 0.1 M phosphate buffer (PB; pH 7.4) overnight at 4 °C. The next day, it was washed three times with 0.1 M PB and cut along the sagittal plane using a vibratome (Leica VT2100S). Serial parasagittal sections (50 mm thick) were cryoprotected in a 30% sucrose solution in PB and stored in ethylene glycol/glycerol at 20 °C until they were analyzed. Regarding the other hemisphere, the hippocampus was rapidly dissected on ice and frozen in liquid nitrogen for other studies.

Immunofluorescence Techniques and Quantifications. For immunofluorescence experiments, three brain sagittal sections between 0.60 and 1.20 mm (approximately) lateral to the midline in Paxinos and Franklin's Mouse Brain Atlas[44] were used. Free-floating serial sections (50 μm thick) were first rinsed in PB and then preincubated for 2 h in PB with 0.25% Triton-X100 and 3% normal serum of the species in which the secondary antibodies were raised (Normal Donkey Serum, Invitrogen, Thermo Scientific). Subsequently, brain sections were incubated for 24h at 4 °C in the same preincubation stock solution (PB + Triton + Serum) containing different combinations of the following primary antibodies: L1516 (Merck) for Lectin from Wisteria floribunda (WFA) and Aggrecan (Merck, ab1031). After rinsing in the sections in PB, they were incubated for 2 h at room temperature in anti-streptavidin Alexa 488 (Thermo Fisher, S-32254) and donkey antirabbit 267 Alexa 594 (Thermo Fisher, A-21207). Sections were also labeled with the nuclear stain DAPI (4,6-diamidino2-phenylindole; Sigma, St. Louis, MO). We obtained stitched image stacks from the entire DG in the hippocampus. These were recorded at 1-μm intervals through separate channels with a 20× lens for the analysis of neurogenesis and the extracellular matrix (ECM). The same range of z-slices was obtained from each slide in each experiment. Adobe Photoshop (CS4) software was used to build the figures.

Immunohistochemical quantifications for perineuronal nets (PNN) of the ECM, were performed by counting positive units labeled with WFA in the DG (including the GCL and hilus) from three consecutive medial brain sections. To determine the density of different cells, the different layers of DG were traced on the DAPI channel of the z projection of each confocal stack of images, and the area of this structure was measured using the freehand drawing tool in Fiji. This area was multiplied by the stack thickness to calculate the reference volume. The number of positive cells was divided by the reference volume, and the density (number of cells/mm3) of cells was calculated.

Behavioral Tests. Open field (OF) and novel object recognition (NOR) tests were performed as described previously.[18] Locomotor activity, as well as anxiety and depression-like behavior, was evaluated using the OF test during a 10 min session. In brief, on the 1st day, the mice were placed individually in a 45 × 45 cm^2 plastic box with vertical opaque walls for 10 min. Each session was recorded, and data such as distance, average speed, and latency to the first entry on the center square of the box were analyzed with the ANY-maze software. The next day, NOR test was performed. The mice were placed in the same box for 5 min and allowed to explore two identical objects: A and B (two black rook chess pieces). The two objects were placed on the long axis of the box, each 13 cm from the end of the box. After each exposure, the objects and the box were wiped with 70% ethanol to eliminate odors that could potentially affect the behavior of

https://doi.org/10.1021/acsomega.4c10849
ACS Omega 2025, 10, 13236−13250

successive mice. Two hours after the familiarization trial, each mouse was released into the box with the same object previously used (object A) and a new one (object C, a tower of colored plastic pieces), instead of object B (short-term memory test). Object C was placed in the same position as object B in the familiarization trial. The mice were allowed 5 min to explore the box. Five days later, the mice were released into the box again, with object A in the same position and another new object (object D, a falcon tube filled with wood chips) in the same position as object C in the previous test. Again, the animals were allowed 5 min to explore the box (long-term memory test). The memory index (MI) was used to measure the recognition memory performance. The MI was defined as the ratio of time spent exploring or the number of entries in the new object (tC or tD) to the time spent exploring both objects (tA + tC or tA + tD) (MI = [tC/(tA + tC)] × 100 and [tD/(tA + tD)] × 100). ANY-maze software was used to calculate the time mice spent exploring the different objects. The animals whose total exploration time of both objects was less than 2 s were excluded. To assess spatial memory, a Y maze test based on published protocols with modifications was used. This test is based on the innate curiosity of rodents to explore novel areas. First, the mice were placed into one of the arms of a black Y-maze apparatus, comprising three plastic arms forming a "Y" shape. They were then allowed to explore the maze for 10 min with one of the arms closed (training trial). After 1 h, the mice were returned to the same arm of the Y maze (start arm) and were allowed to explore all three arms of the maze for 5 min. The number of entries into each arm and the time spent in each arm were registered on video recordings and analyzed by ANY-maze software. We compared the percentage of time spent in the "novel" arm during the whole trial as a measure of spatial memory performance.

Statistical Analysis. The data are presented as mean values ± SEM. Statistical analyses were performed using GraphPad Prism8. The experiments, as well as the acquisition and analysis of all data, were conducted in a randomized order by investigators who were blinded to the experimental conditions. To compare the two experimental groups (mice injected with vehicle or FRα-binding peptide), data were previously tested for normality using the Shapiro-Wilk test, and an unpaired Student's t test was carried out. A one-way ANOVA with Tukey's multiple comparisons test was conducted to study differences in the structure of FRα upon different peptide binding. The Kruskal–Wallis test followed by the uncorrected Dunn's test was used for multiple comparisons and post hoc analysis to analyze in vitro results of Klf4 and Sox2 Yamanaka factors expression. A 95% confidence interval was applied for the statistical comparisons.

■ ASSOCIATED CONTENT

Supporting Information

The Supporting Information is available free of charge at https://pubs.acs.org/doi/10.1021/acsomega.4c10849.

Graphical representation of the protocol followed for the behavioral study of animals subjected to gastric inoculations with either the peptide or vehicle solution (Figure S1) (PDF)

■ AUTHOR INFORMATION

Corresponding Author

Jesus Avila − *Centro de Biologia Molecular Severo Ochoa, CSIC-UAM, 28049 Madrid, Spain; Center for Networked Biomedical Research on Neurodegenerative Diseases (CIBERNED), Instituto de Salud Carlos III, 28029 Madrid, Spain;* orcid.org/0000-0002-6288-0571; Email: javila@cbm.csic.es

Authors

Alejandro Anton-Fernandez − *Centro de Biologia Molecular Severo Ochoa, CSIC-UAM, 28049 Madrid, Spain;* Present Address: Department of Neuroscience and Biomedical Sciences, Carlos III University (UC3M), 28903 Madrid, Spain

Indalo Domene-Serrano − *Centro de Biologia Molecular Severo Ochoa, CSIC-UAM, 28049 Madrid, Spain;* Present Address: Facultad de Ciencias Experimentales, Universidad Francisco de Vitoria, Pozuelo de Alarcon, 28223 Madrid, Spain.

Raquel Cuadros − *Centro de Biologia Molecular Severo Ochoa, CSIC-UAM, 28049 Madrid, Spain; Center for Networked Biomedical Research on Neurodegenerative Diseases (CIBERNED), Instituto de Salud Carlos III, 28029 Madrid, Spain*

Rocio Peinado-Cahuchola − *Centro de Biologia Molecular Severo Ochoa, CSIC-UAM, 28049 Madrid, Spain*

Margarita Sanchez-Pece − *Centro de Biologia Molecular Severo Ochoa, CSIC-UAM, 28049 Madrid, Spain*

Felix Hernandez − *Centro de Biologia Molecular Severo Ochoa, CSIC-UAM, 28049 Madrid, Spain*

Complete contact information is available at: https://pubs.acs.org/10.1021/acsomega.4c10849

Notes

The authors declare no competing financial interest.

■ ACKNOWLEDGMENTS

The authors thank the Advanced Light Microscopy Facility (SMOA). They are also deeply grateful to the Fundación Ramón Areces for their support and to the Centro de Biología Molecular Severo Ochoa (CBM), recognized as a Severo Ochoa Center of Excellence (MICIN, Award CEX2021-001154-S). Special thanks go to Nuria de la Torre Alonso for her technical and editorial assistance. Table of Contents Graphic created in https://BioRender.com.

■ REFERENCES

(1) Bibbins-Domingo, K.; Grossman, D. C.; Curry, S. J.; Davidson, K. W.; Epling, J. W., Jr.; Garcia, F. A.; Kemper, A. R.; Krist, A. H.; Kurth, A. E.; et al. Folic Acid Supplementation for the Prevention of Neural Tube Defects: US Preventive Services Task Force Recommendation Statement. *JAMA* **2017**, *317* (2), 183−189.

(2) Fenech, M. Folate, DNA damage and the aging brain. *Mech. Ageing Dev.* **2010**, *131* (4), 236−241.

(3) Nzila, A.; Ward, S. A.; Marsh, K.; Sims, P. F.; Hyde, J. E. Comparative folate metabolism in humans and malaria parasites (part II): activities as yet untargeted or specific to Plasmodium. *Trends Parasitol.* **2005**, *21* (7), 334−339.

(4) Annibal, A.; Tharyan, R. G.; Schonewolff, M. F.; Tam, H.; Latza, C.; Auler, M. M. K.; Gronke, S.; Partridge, L.; Antebi, A. Regulation of the one carbon folate cycle as a shared metabolic signature of longevity. *Nat. Commun.* **2021**, *12* (1), No. 3486. Bailey, L. B.; Gregory, J. F., 3rd Folate metabolism and requirements. *J. Nutr.* **1999**,

129 (4), 779−782. Ho, C. T.; Shang, H. S.; Chang, J. B.; Liu, J. J.; Liu, T. Z. Folate deficiency-triggered redox pathways confer drug resistance in hepatocellular carcinoma. *Oncotarget* **2015**, *6* (28), 26104−26118.

(5) Kamen, B. A.; Wang, M. T.; Streckfuss, A. J.; Peryea, X.; Anderson, R. G. Delivery of folates to the cytoplasm of MA104 cells is mediated by a surface membrane receptor that recycles. *J. Biol. Chem.* **1988**, *263* (27), 13602−13609. Matherly, L. H.; Goldman, D. I. Membrane transport of folates. *Vitam. Horm.* **2003**, *66*, 403−456. Zhao, R.; Matherly, L. H.; Goldman, I. D. Membrane transporters and folate homeostasis: intestinal absorption and transport into systemic compartments and tissues. *Expert Rev. Mol. Med.* **2009**, *11*, No. e4.

(6) Antony, A. C. Folate receptors: reflections on a personal odyssey and a perspective on unfolding truth. *Adv. Drug Delivery Rev.* **2004**, *56* (8), 1059−1066. Ratnam, M.; Marquardt, H.; Duhring, J. L.; Freisheim, J. H. Homologous membrane folate binding proteins in human placenta: cloning and sequence of a cDNA. *Biochemistry* **1989**, *28* (20), 8249−8254. Shen, F.; Ross, J. F.; Wang, X.; Ratnam, M. Identification of a novel folate receptor, a truncated receptor, and receptor type beta in hematopoietic cells: cDNA cloning, expression, immunoreactivity, and tissue specificity. *Biochemistry* **1994**, *33* (5), 1209−1215.

(7) Chancy, C. D.; Kekuda, R.; Huang, W.; Prasad, P. D.; Kuhnel, J. M.; Sirotnak, F. M.; Roon, P.; Ganapathy, V.; Smith, S. B. Expression and differential polarization of the reduced-folate transporter-1 and the folate receptor alpha in mammalian retinal pigment epithelium. *J. Biol. Chem.* **2000**, *275* (27), 20676−20684. Kamen, B. A.; Smith, A. K. A review of folate receptor alpha cycling and 5-methyltetrahydrofolate accumulation with an emphasis on cell models in vitro. *Adv. Drug Delivery Rev.* **2004**, *56* (8), 1085−1097. Uhlen, M.; Fagerberg, L.; Hallstrom, B. M.; Lindskog, C.; Oksvold, P.; Mardinoglu, A.; Sivertsson, A.; Kampf, C.; Sjostedt, E.; Asplund, A.; et al. Proteomics. Tissue-based map of the human proteome. *Science* **2015**, *347* (6220), No. 1260419.

(8) Bueno, R.; Appasani, K.; Mercer, H.; Lester, S.; Sugarbaker, D. The alpha folate receptor is highly activated in malignant pleural mesothelioma. *J. Thorac. Cardiovasc. Surg.* **2001**, *121* (2), 225−233.

(9) Chen, C.; Ke, J.; Zhou, X. E.; Yi, W.; Brunzelle, J. S.; Li, J.; Yong, E. L.; Xu, H. E.; Melcher, K. Structural basis for molecular recognition of folic acid by folate receptors. *Nature* **2013**, *500* (7463), 486−489.

(10) Wibowo, A. S.; Singh, M.; Reeder, K. M.; Carter, J. J.; Kovach, A. R.; Meng, W.; Ratnam, M.; Zhang, F.; Dann, C. E., 3rd Structures of human folate receptors reveal biological trafficking states and diversity in folate and antifolate recognition. *Proc. Natl. Acad. Sci. U.S.A.* **2013**, *110* (38), 15180−15188.

(11) Boshnjaku, V.; Shim, K. W.; Tsurubuchi, T.; Ichi, S.; Szany, E. V.; Xi, G.; Mania-Farnell, B.; McLone, D. G.; Tomita, T.; Mayanil, C. S. Nuclear localization of folate receptor alpha: a new role as a transcription factor. *Sci. Rep.* **2012**, *2*, No. 980.

(12) Mohanty, V.; Shah, A.; Allender, E.; Siddiqui, M. R.; Monick, S.; Ichi, S.; Mania-Farnell, B.; D, G. M.; Tomita, T.; Mayanil, C. S. Folate Receptor Alpha Upregulates Oct4, Sox2 and Klf4 and Downregulates miR-138 and miR-let-7 in Cranial Neural Crest Cells. *Stem Cells* **2016**, *34* (11), 2721−2732.

(13) Takahashi, K.; Yamanaka, S. Induction of pluripotent stem cells from mouse embryonic and adult fibroblast cultures by defined factors. *Cell* **2006**, *126* (4), 663−676.

(14) Kim, J.; Lengner, C. J.; Kirak, O.; Hanna, J.; Cassady, J. P.; Lodato, M. A.; Wu, S.; Faddah, D. A.; Steine, E. J.; Gao, Q.; et al. Reprogramming of postnatal neurons into induced pluripotent stem cells by defined factors. *Stem Cells* **2011**, *29* (6), 992−1000.

(15) Rodriguez-Matellan, A.; Alcazar, N.; Hernandez, F.; Serrano, M.; Avila, J. In Vivo Reprogramming Ameliorates Aging Features in Dentate Gyrus Cells and Improves Memory in Mice. *Stem Cell Rep.* **2020**, *15* (5), 1056−1066.

(16) Cummings, J.; Scheltens, P.; McKeith, I.; Blesa, R.; Harrison, J. E.; Bertolucci, P. H.; Rockwood, K.; Wilkinson, D.; Wijker, W.; Bennett, D. A.; et al. Effect Size Analyses of Souvenaid in Patients with Alzheimer's Disease. *J. Alzheimers Dis.* **2016**, *55* (3), 1131−1139.

(17) Hulin-Curtis, S. L.; Davies, J. A.; Nestic, D.; Bates, E. A.; Baker, A. T.; Cunliffe, T. G.; Majhen, D.; Chester, J. D.; Parker, A. L. Identification of folate receptor alpha (FRalpha) binding oligopeptides and their evaluation for targeted virotherapy applications. *Cancer Gene Ther.* **2020**, *27* (10−11), 785−798.

(18) Anton-Fernandez, A.; Cuadros, R.; Peinado-Cahuchola, R.; Hernandez, F.; Avila, J. Role of folate receptor alpha in the partial rejuvenation of dentate gyrus cells: Improvement of cognitive function in 21-month-old aged mice. *Sci. Rep.* **2024**, *14* (1), No. 6915.

(19) Ma, P.; Li, D. W.; Bruschweiler, R. Predicting protein flexibility with AlphaFold. *Proteins* **2023**, *91* (6), 847−855.

(20) Xie, N. Z.; Du, Q. S.; Li, J. X.; Huang, R. B. Exploring Strong Interactions in Proteins with Quantum Chemistry and Examples of Their Applications in Drug Design. *PLoS One* **2015**, *10* (9), No. e0137113.

(21) Hayflick, L. A brief history of the mortality and immortality of cultured cells. *Keio J. Med.* **1998**, *47* (3), 174−182.

(22) Aksenova, M. V.; Aksenov, M. Y.; Markesbery, W. R.; Butterfield, D. A. Aging in a dish: age-dependent changes of neuronal survival, protein oxidation, and creatine kinase BB expression in long-term hippocampal cell culture. *J. Neurosci. Res.* **1999**, *58* (2), 308−317.

(23) Lesuisse, C.; Martin, L. J. Long-term culture of mouse cortical neurons as a model for neuronal development, aging, and death. *J. Neurobiol.* **2002**, *51* (1), 9−23.

(24) Inagaki, E.; Yoshimatsu, S.; Okano, H. Accelerated neuronal aging in vitro approximately melting watch approximately. *Front. Aging Neurosci.* **2022**, *14*, No. 868770.

(25) Paoletti, P.; Bellone, C.; Zhou, Q. NMDA receptor subunit diversity: impact on receptor properties, synaptic plasticity and disease. *Nat. Rev. Neurosci.* **2013**, *14* (6), 383−400.

(26) Ge, Y.; Wang, Y. T. GluN2B-containing NMDARs in the mammalian brain: pharmacology, physiology, and pathology. *Front. Mol. Neurosci.* **2023**, *16*, No. 1190324.

(27) Won, S.; Incontro, S.; Nicoll, R. A.; Roche, K. W. PSD-95 stabilizes NMDA receptors by inducing the degradation of STEP61. *Proc. Natl. Acad. Sci. U.S.A.* **2016**, *113* (32), E4736−4744.

(28) Chen, X.; Zhang, Q.; Li, B.; Lu, C.; Yang, S.; Long, J.; He, B.; Chen, H.; Huang, J. BBPpredict: A Web Service for Identifying Blood-Brain Barrier Penetrating Peptides. *Front. Genet.* **2022**, *13*, No. 845747, DOI: 10.3389/fgene.2022.845747.

(29) The UniProt Consortium. UniProt: the Universal Protein Knowledgebase in 2023. *Nucleic Acids Res.* **2022**, *51* (D1), D523−D531.

(30) Zhang, G. Y.; Ma, Z. J.; Wang, L.; Sun, R. F.; Jiang, X. Y.; Yang, X. J.; Long, B.; Ye, H. L.; Zhang, S. Z.; Yu, Z. Y.; et al. The Role of Shcbp1 in Signaling and Disease. *Curr. Cancer Drug Targets* **2019**, *19* (11), 854−862.

(31) Schmandt, R.; Liu, S. K.; McGlade, C. J. Cloning and characterization of mPAL, a novel Shc SH2 domain-binding protein expressed in proliferating cells. *Oncogene* **1999**, *18* (10), 1867−1879.

(32) Zheng, Y.; Zhang, C.; Croucher, D. R.; Soliman, M. A.; St-Denis, N.; Pasculescu, A.; Taylor, L.; Tate, S. A.; Hardy, W. R.; Colwill, K.; et al. Temporal regulation of EGF signalling networks by the scaffold protein Shc1. *Nature* **2013**, *499* (7457), 166−171.

(33) Wills, M. K.; Jones, N. Teaching an old dogma new tricks: twenty years of Shc adaptor signalling. *Biochem. J.* **2012**, *447* (1), 1−16.

(34) Migaud, M.; Charlesworth, P.; Dempster, M.; Webster, L. C.; Watabe, A. M.; Makhinson, M.; He, Y.; Ramsay, M. F.; Morris, R. G.; Morrison, J. H.; et al. Enhanced long-term potentiation and impaired learning in mice with mutant postsynaptic density-95 protein. *Nature* **1998**, *396* (6710), 433−439. Park, C. S.; Elgersma, Y.; Grant, S. G.; Morrison, J. H. alpha-Isoform of calcium-calmodulin-dependent protein kinase II and postsynaptic density protein 95 differentially regulate synaptic expression of NR2A- and NR2B-containing N-methyl-d-aspartate receptors in hippocampus. *Neuroscience* **2008**, *151* (1), 43−55.

https://doi.org/10.1021/acsomega.4c10849
ACS Omega 2025, 10, 13236−13250

(35) Shimada, A.; Keino, H.; Satoh, M.; Kishikawa, M.; Hosokawa, M. Age-related loss of synapses in the frontal cortex of SAMP10 mouse: a model of cerebral degeneration. *Synapse* **2003**, *48* (4), 198−204.
(36) Caly, A.; Sliwinska, M. A.; Ziolkowska, M.; Lukasiewicz, K.; Pagano, R.; Dzik, J. M.; Kalita, K.; Bernas, T.; Stewart, M. G.; Giese, K. P.; et al. PSD-95 in CA1 Area Regulates Spatial Choice Depending on Age. *J. Neurosci.* **2021**, *41* (11), 2329−2343. Ni, M. Z.; Zhang, Y. M.; Li, Y.; Wu, Q. T.; Zhang, Z. Z.; Chen, J.; Luo, B. L.; Li, X. W.; Chen, G. H. Environmental enrichment improves declined cognition induced by prenatal inflammatory exposure in aged CD-1 mice: Role of NGPF2 and PSD-95. *Front. Aging Neurosci.* **2022**, *14*, No. 1021237. Rogers, N. T.; Steptoe, A.; Cadar, D. Frailty is an independent predictor of incident dementia: Evidence from the English Longitudinal Study of Ageing. *Sci. Rep.* **2017**, *7* (1), No. 15746.
(37) Anton-Fernandez, A.; Roldan-Lazaro, M.; Valles-Saiz, L.; Avila, J.; Hernandez, F. In vivo cyclic overexpression of Yamanaka factors restricted to neurons reverses age-associated phenotypes and enhances memory performance. *Commun. Biol.* **2024**, *7* (1), 631.
(38) Mitchell, W.; Goeminne, L. J. E.; Tyshkovskiy, A.; Zhang, S.; Chen, J. Y.; Paulo, J. A.; Pierce, K. A.; Choy, A. H.; Clish, C. B.; Gygi, S. P.; et al. Multi-omics characterization of partial chemical reprogramming reveals evidence of cell rejuvenation. *eLife* **2024**, *12*, No. e90579, DOI: 10.7554/eLife.90579. Roux, A. E.; Zhang, C.; Paw, J.; Zavala-Solorio, J.; Malahias, E.; Vijay, T.; Kolumam, G.; Kenyon, C.; Kimmel, J. C. Diverse partial reprogramming strategies restore youthful gene expression and transiently suppress cell identity. *Cell Syst.* **2022**, *13* (7), 574−587.
(39) Chaunsali, L.; Tewari, B. P.; Sontheimer, H. Perineuronal Net Dynamics in the Pathophysiology of Epilepsy. *Epilepsy Curr.* **2021**, *21* (4), 273−281. Romberg, C.; Yang, S.; Melani, R.; Andrews, M. R.; Horner, A. E.; Spillantini, M. G.; Bussey, T. J.; Fawcett, J. W.; Pizzorusso, T.; Saksida, L. M. Depletion of perineuronal nets enhances recognition memory and long-term depression in the perirhinal cortex. *J. Neurosci.* **2013**, *33* (16), 7057−7065.
(40) Baek, M.; DiMaio, F.; Anishchenko, I.; Dauparas, J.; Ovchinnikov, S.; Lee, G. R.; Wang, J.; Cong, Q.; Kinch, L. N.; Schaeffer, R. D.; et al. Accurate prediction of protein structures and interactions using a three-track neural network. *Science* **2021**, *373* (6557), 871−876.
(41) Mirdita, M.; Schutze, K.; Moriwaki, Y.; Heo, L.; Ovchinnikov, S.; Steinegger, M. ColabFold: making protein folding accessible to all. *Nat. Methods* **2022**, *19* (6), 679−682.
(42) Green, P. S.; Bishop, J.; Simpkins, J. W. 17 alpha-estradiol exerts neuroprotective effects on SK-N-SH cells. *J. Neurosci.* **1997**, *17* (2), 511−515.
(43) Ritter, M. L.; Avila, J.; Garcia-Escudero, V.; Hernandez, F.; Perez, M. Frontotemporal Dementia-Associated N279K Tau Mutation Localizes at the Nuclear Compartment. *Front. Cell. Neurosci.* **2018**, *12*, 202.
(44) Paxinos, G.; Franklin, K. *Paxinos and Franklin's the Mouse Brain in Stereotaxic Coordinates*; Elsevier Ltd., 2019.

https://doi.org/10.1021/acsomega.4c10849
ACS Omega 2025, 10, 13236−13250